Estimating Steady-State Evaporation Rates From Bare Soils Under Conditions of High Water Table

Estimating Steady-State Evaporation Rates From Bare Soils Under Conditions of High Water Table

By C. D. RIPPLE, JACOB RUBIN, *and* T. E. A. VAN HYLCKAMA

TECHNIQUES IN UNSATURATED-ZONE HYDROLOGY

CONTENTS

ILLUSTRATIONS

SYMBOLS

---

a = a subscript, indicating a variable determined in the air, H_a centimeters above the soil surface.

A = sensible heat transfer into the air, calories per centimeter^2 per day (cal cm^{-2} day^{-1}).

b = $-B(T_u - T_1)/L_u{}^*$, grams per centimeter^4 (gm cm^{-4}).

B = $(\eta/\sigma)\,(\check{r}/\alpha)\,\beta'$, grams per centimeter^3 per degree kelvin (gm cm^{-3} °K^{-1}).

c = E/D_{hv}, centimeters^{-1}.

D_a = a coefficient characterizing the molecular diffusion of water vapor in free air, centimeters^2 per day (cm^2 day^{-1}).

D_{hv} = a coefficient characterizing the molecular diffusion of soil-water vapor caused by humidity gradients, centimeters^2 per day (cm^2 day^{-1}).

D_{Tv} = a coefficient characterizing the molecular diffusion of soil-water vapor caused by thermal gradients, centimeters^2 per day per degree Kelvin (cm^2 day^{-1} °K^{-1}).

e = E/K_{sat}, rate of evaporation from the soil, dimensionless.

E = rate of evaporation from the soil, centimeters per day (cm day^{-1}).

e_{pot} = rate of potential evaporation, dimensionless.

E_{pot} = rate of potential evaporation, centimeters per day (cm day^{-1}).

e_∞ = soil-limited rate of evaporation from the soil, dimensionless.

E_∞ = soil-limited rate of evaporation from the soil, centimeters per day (cm day^{-1}).

$f(e)$ = a functional relation defined by equation 27.

F_m = a function which relates E and S_u, using meteorological parameters.

F_g = a function which relates E and S_u, using soil parameters.

g = acceleration of gravity = 980 centimeters per second^2 (cm sec^{-2}).

$G(V_a)$ = a theoretically or empirically derived known function of wind speed, centimeters per day per millibar (cm day^{-1} mb^{-1}).

h = relative humidity, dimensionless.

h_a = air relative humidity at height H_a above the soil surface, dimensionless.

H_a = height of meteorological measurements above the soil surface, centimeters.

h_u = surface-soil relative humidity, dimensionless.

H_u = roughness parameter, centimeters (usually, for bare soils, $0.01 \leq H_u \leq 0.03$).

h_1 = soil relative humidity at depth L_u, dimensionless.

$h_1{}^*$ = soil relative humidity at depth $L_u{}^*$, dimensionless.

$I(y)$ = the integral relation defined by the right-hand side of equation 18.

k = von Karman constant = 0.41, dimensionless.

K = K_{liq} = hydraulic conductivity for liquid flow, centimeters per day (cm day^{-1}).

K_{sat} = hydraulic conductivity of water-saturated soil, centimeters per day (cm day^{-1}).

K_{vap} = hydraulic conductivity for vapor flow, centimeters per day (cm day^{-1}).

l = $L/S_{1/2}$, depth to water table, dimensionless.

L = total distance between the water table and soil surface, centimeters.

L_j = in the multilayer case, the thickness of soil layer, centimeters, j layers above the water table (that is, $j = 1$ means one layer above the water table, and so forth).

L_u = thickness of the uppermost soil layer, centimeters.

$L_u{}^*$ = thickness of the uppermost portion of the dry soil surface at which T_1 was determined, centimeters.

L_u' = thickness of the dry soil layer in which isothermal vapor transfer is assumed to predominate, centimeters.

M = molecular weight of water = 18 grams per mole (gm mol^{-1}).

n = an integer soil coefficient which usually ranges from 2 for clays to 5 for sands.

p = saturation vapor pressure of water, millibars.

$p(T)$ = a known relation between the saturation water-vapor pressure and temperature (given in tabular or functional form), millibars.

P = ambient pressure, millibars (taken as $P = 1,000$ mb in this study).

q = flux of water, centimeters per day (cm day^{-1}).

Q_g = soil heat flux into the ground, calories per centimeter^2 per day (cal cm^{-2} day^{-1}).

Q_N = net radiative flux received by the soil surface, calories per centimeter^2 per day (cal cm^{-2} day^{-1}).

R = gas constant $= 8.32 \times 10^7$ ergs per degree Kelvin per mole (erg °K^{-1} mole^{-1}).

s = $S/S_{1/2}$, dimensionless suction.

S = soil-water suction, defined as the negative of the soil-water pressure head, centimeters of water.

S_j = in the multilayer case, the soil-water suction at the upper interface of layer j, centimeters of water.

S_u = water suction at the soil surface, centimeters of water.

$S_{1/2}$ = a constant soil coefficient representing S at $K = \frac{1}{2} K_{sat}$, centimeters of water.

T = temperature, degrees Kelvin (°K).

T_a = air temperature at H_a, degrees Kelvin (°K).

T_u = surface soil temperature, degrees Kelvin (°K).

T_1 = soil temperature at depth L_u^*, degrees Kelvin (°K).

u = a subscript, indicating a variable determined at the soil surface.

v = a subscript, indicating a variable which involves water-vapor transfer.

V_a = wind speed at height H_a, centimeters per day (cm day^{-1}).

y = a variable, defined by equation 16.

$\tilde{y}$ = a variable, defined in conjunction with the right-hand side of equation 31 of the layered-soil case.

z = $Z/S_{1/2}$, height above water table, dimensionless.

Z = vertical height above the water table, centimeters.

α = tortuosity factor, dimensionless.

β' = $d(\log_e \rho_v)/dT$, grams per centimeter^3 per degree Kelvin (gm cm^{-3} °K^{-1}).

γ = psychrometric constant $= 0.000659\ P$, millibars per degree Kelvin (mb °K^{-1}).

ϵ = water/air molecular ratio $= 0.622$ (dimensionless).

ζ = a ratio of the average temperature gradient in the air-filled soil pores to the overall soil temperature gradient, dimensionless.

η = soil porosity, dimensionless.

λ = latent heat of vaporization of water at T_a, calories per gram (cal gm^{-1}).

ρ_a = air density at T_a, grams per centimeter^3 (gm cm^{-3}).

ρ_v = $\rho_v(T)$ = density of saturated water vapor, grams per centimeter^3 (gm cm^{-3}); ρ_v is a function of temperature.

ρ_w = water density at appropriate T, grams per centimeter^3 (gm cm^{-3}).

σ = volumetric air content of the soil, dimensionless.

$\Phi(\sigma)$ = a function defining the effectiveness of the water-free pore space for diffusion, dimensionless.

ESTIMATING STEADY-STATE EVAPORATION RATES FROM BARE SOILS UNDER CONDITIONS OF HIGH WATER TABLE

By C. D. Ripple, Jacob Rubin, and T. E. A. van Hylckama

ABSTRACT

A procedure that combines meteorological and soil equations of water transfer makes it possible to estimate approximately the steady-state evaporation from bare soils under conditions of high water table. Field data required include soil-water retention curves, water-table depth, and a record of air temperature, air humidity, and wind velocity at one elevation. The procedure takes into account the relevant atmospheric factors and the soil's capability to conduct water in liquid and vapor forms. It neglects the effects of thermal transfer (except in the vapor case) and of salt accumulation. The evaporation rate can be estimated for homogeneous as well as layered soils. Results obtained with the method demonstrate how the soil-water evaporation rates depend on potential evaporation, water table depth, vapor transfer, and certain soil parameters.

INTRODUCTION

It is sometimes desirable to estimate the evaporation rates from bare land surfaces and to predict approximately the variation of these rates with meteorological conditions or with man-imposed changes in the water-table level. This estimate might be rather important in certain regions during the appraisal of ground-water availability. For such purposes, it is often both permissible and useful to use relatively simple estimation methods. One possibility is to assume steady state of the hydraulic-gradient-driven upward flux of water and to neglect certain effects of soil temperature and of solute accumulations.

The basic approaches required for the development of this method can be found in the literature. Gardner (1958) suggested a convenient equation for describing hydraulic conductivity, the most relevant soil parameter, and from it developed methods for evaluating soil-limited evaporation in cases of high water table. Arbhabhirama, Duke, and Corey (1965) and Stallman (1967) employed Gardner's general approach but

used different soil parametric equations. They demonstrated the usefulness of dimensionless curves in solving problems of the type under consideration.

The above treatments stressed the cases in which soil properties were the determining factor of evaporation. Cases of evaporation in which the atmospheric conditions play the decisive role can be treated by means of several purely meteorological equations (for example, Slatyer and McIlroy, 1961).

Philip (1957a, b) showed how the effects of the soil factors on bare-soil evaporation interacted with the effects of the atmospheric parameters on bare-soil evaporation. Owing to his utilization of numerical methods, Philip's approach to soil influences was more general but mathematically less convenient than Gardner's approach.

All the studies quoted above concerned themselves with homogeneous soils and mainly with cases involving liquid transfer. Gardner indicated how to include the vapor-transfer effects, but only for selected circumstances. Philip's approach to vapor effects is more general, but again mathematically less convenient.

The purpose of this paper is to integrate and extend the above approaches for estimating steady-state evaporation from bare soils under high water-table conditions. The past approaches are unified, modified, and supplemented when necessary to improve their practicability as a general (though approximate) method.

Stress has been placed on use of readily available data, simple parameter-determination techniques, dimensionless variables, and simple graphical or algebraic treatments. Numerical integrations have been avoided. The older approaches are generalized so as to make them applicable to layered as well as homogeneous soils. In addition, analysis of the multilayer case is modified to allow for the treatment of evaporation affected by water-vapor transfer. Examples of the results obtained with the suggested method are presented, discussed, and utilized for demonstrating the role of some of the relevant factors.

THEORY

The steady-state evaporative fluxes across the boundary between any given soil-atmosphere system may be described by two functional relations. The first deals with the fluxes leaving the soil surface and entering the atmosphere. It may be represented by the meteorological equation

$$S_u = F_m(E). \tag{1}$$

The second describes the fluxes between the water table and the soil surface and may be expressed by the soil equation

$$L = F_g(S_u, E). \tag{2}$$

In the above equations,

L = total distance between the water table and the soil surface, cm,

S_u = water suction at the soil surface, defined as the negative of the soil-water pressure head, cm of water,

E = rate of evaporation from the soil, cm day^{-1},

F_g = a function which relates E and S_u, using soil parameters, and

F_m = a function which relates E and S_u, using meteorological parameters.

Each of the above relations is an algebraic equation containing the same variables, E and S_u. Therefore, the equations can be solved simultaneously to yield values of the actual E and S_u. The determination of the actual E is the main concern of this paper.

METEOROLOGICAL EQUATION

A relation is sought to express meteorological equation 1. For simplicity and ease of handling, however, it is best to treat the components of this relation individually.

The basic meteorological equation used is of the type generally known as the bulk aerodynamic, or Dalton, equation (Slatyer and McIlroy, 1961). Its form is

$$E = G(V_a)[p(T_u)h_u - p(T_a)h_a], \qquad (3)$$

where

$G(V_a)$ = a theoretically or empirically derived known function of wind speed, cm day^{-1} mb^{-1},

V_a = wind speed at height H_a, cm day^{-1},

h = relative humidity, dimensionless,

T = temperature, °K,

p = saturation vapor pressure of water, mb,

$p(T)$ = a known relation between the saturation water-vapor pressure and temperature (given in tabular or functional form), mb,

a = a subscript indicating a variable determined in the air, H_a cm above the soil surface, and

u = a subscript indicating a variable determined at the soil surface.

This equation, owing to its simplicity, has been used extensively for estimating the loss of water by free-water surfaces, plants, and bare soils. Either its empirical form (Harbeck, 1962) or one of its modified forms (Slatyer and McIlroy, 1961, p. 3–40 to 3–44) can be employed.

The present study utilized the wind function used by van Bavel (1966),

$$G(V_a) = \left(\frac{\rho_a \epsilon k^2}{\rho_w P}\right) \frac{V_a}{(\log_e H_a/H_u)^2}, \qquad (4)$$

where

ρ_a = air density at T_a, gm cm^{-3},

ρ_w = water density at T_a gm cm^{-3},

ϵ = water/air molecular ratio = 0.622, dimensionless,

k = von Karman constant = 0.41, dimensionless,

P = ambient pressure, mb (taken as $P = 1,000$ mb in this study),

H_a = height of meteorological measurements, above the soil surface, cm, and

H_u = roughness parameter, cm (usually, for bare soils, $0.01 \leq H_u \leq 0.03$).

Equation 3 may be rewritten as follows to obtain the form required by equation 1

$$h_u = \frac{1}{p(T_u)}\left[\frac{E}{G(V_a)} + p(T_a)h_a\right]. \tag{5}$$

The surface relative humidity, h_u, specified by equation 5 may now be substituted into the thermodynamic relation (Edlefson and Anderson, 1943),

$$S_u = -\frac{RT_u}{Mg}\log_e h_u, \tag{6}$$

where

M = molecular weight of water = 18 gm mole^{-1},

g = acceleration of gravity = 980 cm sec^{-2}, and

R = gas constant = 8.32×10^7 erg °K^{-1} mole^{-1}.

The above substitution would result in an equation expressing S_u in terms of atmospheric variables, the soil surface temperature T_u, and E.

To completely attain the form of equation 1, the variables on the right-hand side of the equation sought should be, except for E, entirely meteorological. But T_u, the surface soil temperature, is present in the combination of equations 5 and 6. To replace T_u with meteorological variables and parameters, an appropriate expression for T_u may be developed. First, note that T_u is related to sensible heat transfer in the air by the following equation for turbulent transfer (Slatyer and McIlroy, 1961, p. 3–53; van Bavel, 1966, p. 466):

$$A = -\lambda\gamma G(V_a)(T_u - T_a), \tag{7}$$

where

A = sensible heat transfer into the air, cal cm^{-2} day^{-1},

λ = latent heat of vaporization of water at T_a, cal gm^{-1}, and

γ = psychrometric constant = $0.000659P$, mb °K^{-1}.

Second, substitute A into the following heat-balance equation (Slatyer and McIlroy, 1961, p. 3–50; van Bavel, 1966, p. 456):

$$Q_N = \lambda\rho_w E + \rho_w A + Q_g, \tag{8}$$

where

> Q_N = net radiative flux received by the soil surface, cal cm^{-2} day^{-1} and
> Q_g = soil heat flux into the ground, cal cm^{-2} day^{-1} (assumed to equal zero for periods of interest in this study).

The combined equations 7 and 8, after rearrangement, yield the following for T_u:

$$T_u = T_a + \frac{Q_N - Q_g - \lambda\rho_w E}{\lambda\gamma\rho_w G(V_a)} . \tag{9}$$

If equation 9 were substituted into a combination of equations 5 and 6, the overall meteorological equation, equivalent to equation 1, would be obtained.

SOIL EQUATION

The simplest system to be considered is shown in figure 1, case A. A homogeneous soil is underlain by a shallow water table, with the reference height Z measured positively upward from the piezometric surface. The soil surface is at $Z = L$.

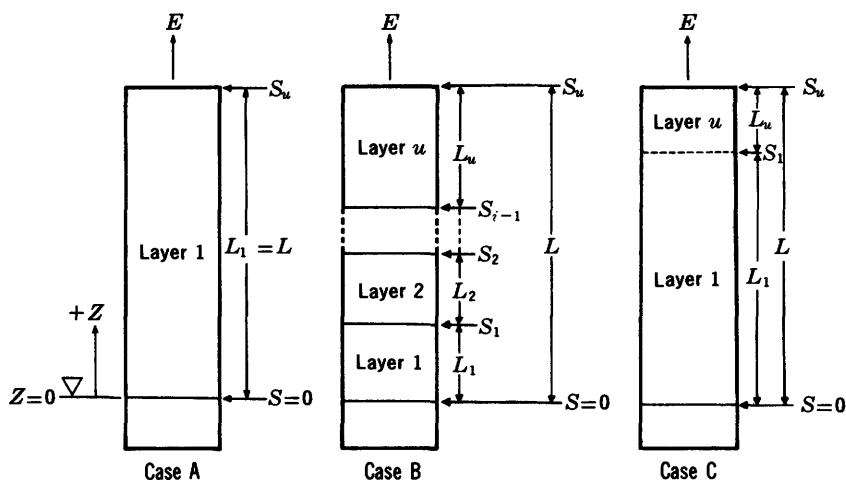FIGURE 1.—Water-table–soil–atmosphere systems considered. Case A: A homogeneous soil in which water is transferred exclusively in liquid form. Case B: A layered soil in which water is transferred exclusively in liquid form. Case C: A homogeneous soil in which water is transferred in liquid and vapor forms, the former transfer being predominant in the lower layer and the later predominant in the upper layer.

For determining water transfer in liquid form, the soil's hydraulic-conductivity relation is assumed to conform to an empirical function, originally suggested by Gardner (1958, equation 11). It is presented here in a modified form (Gardner, 1964) which demonstrates more clearly the physical significance of the coefficients:

$$K = K(S) = \frac{K_{sat}}{\left(\dfrac{S}{S_{1/2}}\right)^n + 1}, \tag{10}$$

where

K = hydraulic conductivity for liquid flow, cm day^{-1},

K_{sat} = hydraulic conductivity of water-saturated soil, cm day^{-1},

S = soil-water suction, defined as the negative of the soil-water pressure head, cm of water,

$S_{1/2}$ = a constant coefficient representing S at $K = \frac{1}{2}K_{sat}$, cm of water, and

n = an integer soil coefficient which usually ranges from 2 for clays to 5 for sands.

Assuming that Darcy's equation holds for flow in both saturated and unsaturated soils, the flux, q, which under steady-state conditions must equal the evaporation rate E, may be described by

$$q = E = K\left(\frac{dS}{dZ} - 1\right). \tag{11}$$

On rearranging and integrating, equation 11 becomes

$$Z' = \int_0^{Z'} dZ = \int_0^{S'} \frac{dS}{\dfrac{E}{K(S)} + 1}, \tag{12}$$

where

$S' = S$ at $Z = Z' \leq L.$

Equation 12 with equation 10 substituted for $K(S)$ becomes

$$Z' = \int_0^{S'} \frac{dS}{\dfrac{E}{K_{sat}}\left[\left(\dfrac{S}{S_{1/2}}\right)^n + 1\right] + 1}. \tag{13}$$

The above integral can be expressed in closed form (Gardner, 1958). Equation 13 expresses explicitly Z' as a function of S and E. Also, it defines implicitly the relation between E and S' for any given Z'. Both

facts have been utilized in the past (Philip, 1957a; Gardner, 1958). Utilization of the implicit relation, however, is unwieldy in practice, except for $n = 1$ or 2, in which case the relation can easily be inverted and made explicit. To convert equation 13 to a more tractable form, the following transformations may be carried out. First, define the dimensionless variable,

$$e = E/K_{sat}, \tag{14}$$

and substitute it into equation 13,

$$Z' = \frac{1}{e} \int_0^{S'} \frac{dS}{\left(\dfrac{S}{S_{1/2}}\right)^n + \left(1 + \dfrac{1}{e}\right)} = \frac{1}{e\left(1 + \dfrac{1}{e}\right)} \int_0^{S'} \frac{dS}{\left[\dfrac{S/S_{1/2}}{\left(1 + \dfrac{1}{e}\right)^{1/n}}\right]^n + 1}. \tag{15}$$

Second, define a variable y by

$$y = \frac{S/S_{1/2}}{\left(1 + \dfrac{1}{e}\right)^{1/n}} = \frac{S}{S_{1/2}}\left(\frac{e}{1+e}\right)^{1/n} \tag{16}$$

and transform the integral of equation 15 with its aid to obtain, after rearrangement, the basic equation of this study,

$$(e+1)\left(\frac{e}{e+1}\right)^{1/n} \frac{Z'}{S_{1/2}} = \int_0^{y'} \frac{dy}{y^n + 1}, \tag{17}$$

where

$$y' = \frac{S'}{S_{1/2}}\left(\frac{e}{e+1}\right)^{1/n}$$

In particular, at the soil surface, when $Z' = L$

$$(e+1)\left(\frac{e}{e+1}\right)^{1/n} \frac{L}{S_{1/2}} = \int_0^{y_u} \frac{dy}{y^n + 1}, \tag{18}$$

where

$$y_u = \frac{S_u}{S_{1/2}}\left(\frac{e}{e+1}\right)^{1/n}$$

The integral on the right-hand side of equations 17 and 18 is known in closed form for any positive n (Gradshteyn and Ryzhik, 1965, equation 2.142). The form of equations 17 or 18 makes it possible to determine the relation between e and the suction (either S' or S_u) for any n by

means of simple graphs. This technique as well as the results obtained with its aid will be described presently.

For certain purposes, the use of equations 17 and 18 can be further simplified by adopting the dimensionless variables

$$s = \frac{S}{S_{1/2}},\qquad(19)$$

$$z = \frac{Z}{S_{1/2}},\qquad(20)$$

and

$$l = \frac{L}{S_{1/2}},\qquad(21)$$

in addition to the dimensionless $e = E/K_{sat}$ used previously. With the exception of s, these dimensionless variables are similar to those employed by Staley (cited by Arbhabhirama and others, 1965), whose hydraulic-conductivity equation is also somewhat similar to equation 10. Inspection of numerous curves indicates that $S_{1/2}$ of the dimensionless s matches the observed relations between K and S better than does the air entry pressure used in this connection by Staley. The above dimensionless variables reduce the basic equation 18 to

$$(e+1)\left(\frac{e}{e+1}\right)^{1/n} l = \int_0^{y_u} \frac{dy}{y^n+1},\qquad(22)$$

where

$$y_u = s_u \left(\frac{e}{e+1}\right)^{1/n}.$$

An analogous reduction can be carried out for equation 17.

The following reasoning leads to another useful relation which is implied by equation 18. It is clear from physical considerations that an increase in the evaporative capacity of the atmosphere will produce an increased suction at the soil surface. This higher suction, in turn, must magnify the upward water flux through the soil. If equation 18 correctly describes reality, such a flux cannot increase without bound, because as S_u (and hence y_u) approaches infinity, the integral on the right-hand side of equation 18 approaches a finite limit, $\pi/(n \sin \pi/n)$ (Gradshteyn and Ryzhik, 1965, equation 3.241–2 with $\mu=1$). It follows that a limiting soil-water flux and hence a soil-limited evaporation, e_∞, exists. For any

particular soil system the latter is given by

$$(e_\infty+1)\left(\frac{e_\infty}{e_\infty+1}\right)^{1/n}\frac{L}{S_{1/2}}=\frac{\pi}{n\sin\dfrac{\pi}{n}} \tag{23}$$

or, in completely dimensionless form,

$$(e_\infty+1)\left(\frac{e_\infty}{e_\infty+1}\right)^{1/n}l=\frac{\pi}{n\sin\dfrac{\pi}{n}}. \tag{24}$$

The last two equations can be simplified considerably if $e_\infty\ll1$ (that is, if $E\ll K_{sat}$). In such a case, $e_\infty+1\cong1$, and equations 23 and 24 lead to

$$E_\infty\cong K_{sat}\left[\frac{S_{1/2}}{L}\right]^n\left[\frac{\pi}{n\sin\dfrac{\pi}{n}}\right]^n \tag{25}$$

and

$$e_\infty\cong\frac{1}{l^n}\left[\frac{\pi}{n\sin\dfrac{\pi}{n}}\right]^n \tag{26}$$

Equation 25 is similar to the formulas for E_{Lim} given without derivation by Gardner (1958) for $n=\frac{3}{2}$, 2, 3, 4 and yields identical numerical coefficients.

APPLICATION

DATA REQUIRED

The equations presented above may be used to compute the estimated evaporation from bare soils under high water-table conditions. The data generally needed for such computations are as follows.

The meteorological data (those needed in connection with the utilization of equations 4, 5, and 9) are obtained by standard techniques or from references. These data include wind velocity, V_a, air temperature, T_a, the air relative humidity, h_a, and net radiation, Q_N. The magnitude of $p(T_a)h_a$, the water-vapor pressure in the air, is determined from T_a and h_a with the aid of standard tables or formulas. Daily Q_N values may be determined either by direct measurement or by the method outlined in

Slatyer and McIlroy (1961, appendix 2). For a given site, the latter technique can produce calculated Q_N values with the aid of standard information in the Smithsonian meteorological tables (List, 1951). A zero value has been assumed for Q_g in the computations of this paper. This is a reasonable assumption for daily means of Q_g, especially when these are used in conjunction with Q_N and $\lambda \rho_w E$. (See equation 9.)

In addition to the above strictly meteorological data, the soil-surface temperature, T_u, is useful because it appears in equations 5 and 6. Data on this temperature are usually unavailable, and thus the development of equation 9 as an indirect method for T_u determination is necessary. If, however, soil-surface temperature data are available, it is possible to avoid the use of equation 9 and of the usually approximate Q_N data needed in connection with this equation.

The soil equation requires knowledge of the hydraulic conductivity for a reasonable range of soil-water suctions. Such data will allow evaluation of the necessary coefficients K_{sat}, n, and $S_{1/2}$ for a particular soil. K_{sat} can be measured directly and readily; however, the other two coefficients are more difficult to obtain. They may be computed from more routinely available data, by using the technique of Marshall (1958), as modified by Millington and Quirk (1961) and by Jackson, Reginato, and van Bavel (1965). This technique produces, for selected magnitudes of S, a series of scaled hydraulic-conductivity values $K'(S) = \xi K(S)$, where ξ is the scale factor and where $K'(S)$ at $S=0$ is designated by K'_{sat}. Note that the scale factor need not be determined to find n and $S_{1/2}$. If equation 10 is obeyed, a plot of $\log (K_{sat}/K(S) - 1) [= \log (K'_{sat}/K'(S) - 1)]$ versus $\log S$ is linear. The slope of such a plot is equal to n, and the plot's intercept with the abscissa determines $S_{1/2}$.

The manner of the computation of the scaled hydraulic-conductivity values is adequately described in the above references. The basic information required by these computations is the characteristic relation between the soil-water suction and the volumetric moisture content (that is, the water-retention curve or the pore-size distribution function). Such data are regularly determined in soil laboratories. Some of these may also be obtained in the field by measuring the moisture content of the soil overlying a sufficiently shallow water table as a function of depth, after a prolonged period of negligible soil-water fluxes.

HOMOGENEOUS SOIL

For a homogeneous soil with insignificant vapor transfer (fig. 1, case A), evaporation, E, can be computed from the meteorological and soil equations in several ways. In most cases it is convenient to compute e first. When appropriate, e may be converted to E by using equation 14. In the early stages of the computation, the soil-imposed upper bounds

of $e(e_\infty)$ or the bounds imposed by atmospheric factors (e_{pot}) may be needed. They can be easily computed as will be shown presently.

Equations 4, 5, 6, and 9 are combined and yield an overall meteorological equation, which expresses S_u as a function of e and which corresponds to equation 1. This equation is substituted into the soil equation 18 to yeild a nonlinear algebraic equation in e. The root of this equation may be found by routine numerical methods. In this study, the method of "false position" (Hildebrand, 1956, p. 446–447) was programmed for a digital computer, tried, and found satisfactory.

Alternately, e can be obtained by plotting the curves corresponding to the above meteorological and soil equations; the magnitude of the actual e is given by the intercept of the two curves. The meteorological equation is plotted for selected values of $e < e_{pot}$ in a straightforward manner. The soil curve is determined for selected values of $e < e_\infty$ by using the following graphical procedure. Any given e value may be used with an appropriate (that is, proper n) plot of

$$f = f(e) = (e+1)\left(\frac{e}{e+1}\right)^{1/n} \tag{27}$$

to determine the corresponding value of f (fig. 2). When f is multiplied by $l = L/S_{1/2}$, one obtains the magnitude of the left-hand side of equation 18. This magnitude is equal to the value of the integral, $I = I(y_u)$, on the right-hand side of the same equation. Then by using a plot of $I(y_u)$, given in figure 3, y_u is found. Finally, the required S_u is computed from y_u by using the relevant definition, given below equation 18.

For less accurate but quicker estimates of the soil curve, dimensionless plots of the type illustrated in figure 4 may be used, in which the needed values of e and s are obtained for any given $z = l$. The limited range covered by the plot and the necessity for a field filled with many curves are the obvious detriments of this approach. It should be noted that the curves in question also indicate the suction within the soil profile as a function of depth for any given evaporation rate.

Exact and approximate limiting evaporation rates, imposed by soil e_∞ or E_∞, can be obtained from equations 23 through 26. The approximate values are given directly by the appropriate equations. The exact values can be computed easily with the aid of figure 2, or if less accurate values are needed, they can be read off directly from an appropriate dimensionless plot in figure 5.

The limiting evaporation rates imposed by meteorological conditions, e_{pot}, can be computed (graphically or numerically) for any weather data by solving simultaneously equations 5 and 9, with $h_u = 1.0$ (that is, with $S_u = 0$).

Examples of results obtained with the aid of the above graphical methods are shown in figures 6, 7, and 8. The examples refer to two selected soils, Chino clay with $n=2$, $S_{1/2}=24$, and $K_{sat}=1.95$ (Gardner and Fireman, 1958) and a coarse-textured alluvial soil taken from the 50–60-cm zone of U.S. Geological Survey evaporation tanks near Buckeye,
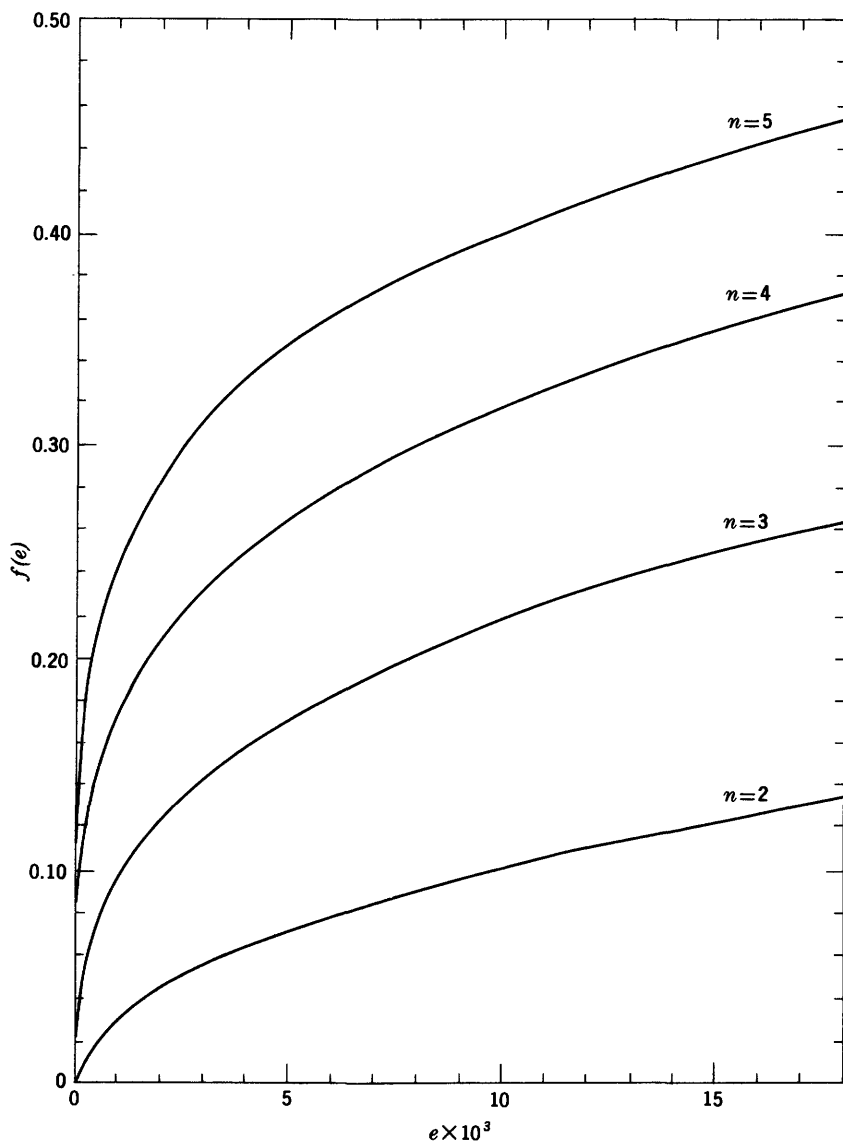

FIGURE 2.—Plots of $f=f(e)=(e+1)\left(\dfrac{e}{e+1}\right)^{1/n}$ for $n=2,\ 3,\ 4,\ 5$.

Ariz., with $n=5$, $S_{1/2}=44.7$, and $K_{sat}=417$. These evaporation tanks are described by van Hylckama (1966).

Application of the graphical intersection method is illustrated in figure 6. The figure shows meteorological curves for several arbitrarily selected atmospheric conditions and soil curves corresponding to several water-table depths. Note that the soil curves approach a limiting E with increasing S_u and thus are in agreement with the previously presented theoretical proof. The rate of approach to the actual E_∞ (or e_∞) shown by the soil curves mainly depends on the value of n characterizing the particular soil. A relatively rapid approach is exhibited by the Buckeye soil $(n=5)$, while the approach of the Chino clay $(n=2)$ is much more gradual. It should be noted that most of the field soils commonly found show n values which lie between 2 and 5. Hence, such soils will usually yield $E(S_u)$ plots similar to or intermediate between those shown in figure 6. The meteorological curves also seem to approach a limiting E, but with decreasing S. The values of E, fixed by the intersection points between meteorological and soil curves of the figures in question, represent the actual evaporation rates under the particular meteorological, soil, and water-table conditions.

The dependence of the actual E on weather and water-table depth is demonstrated more clearly in figures 7 and 8. Figure 7 is concerned with the influence of the depth to water table under given meteorological
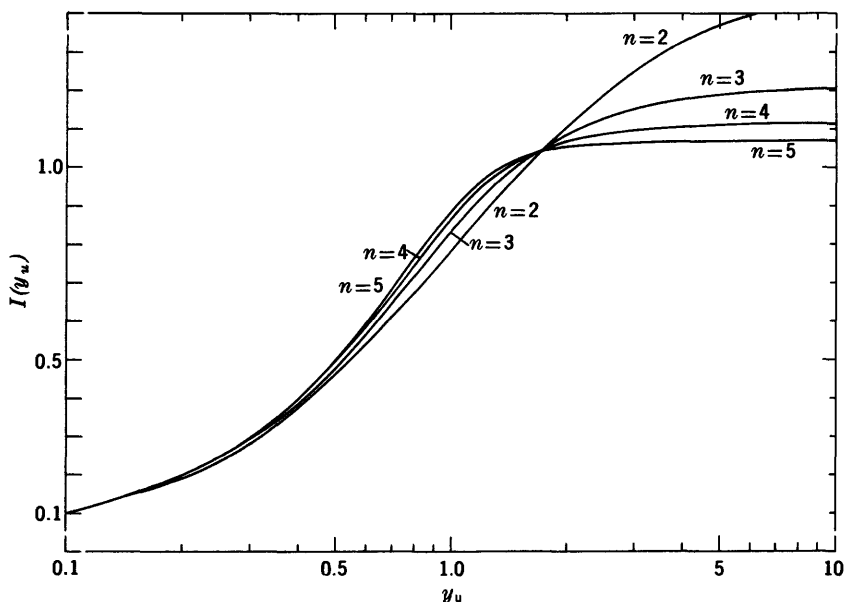
FIGURE 3.—Plots of $I = I(y_u) = \int_0^{y_u} \dfrac{dy}{y^n+1}$ for $n=2, 3, 4, 5$.
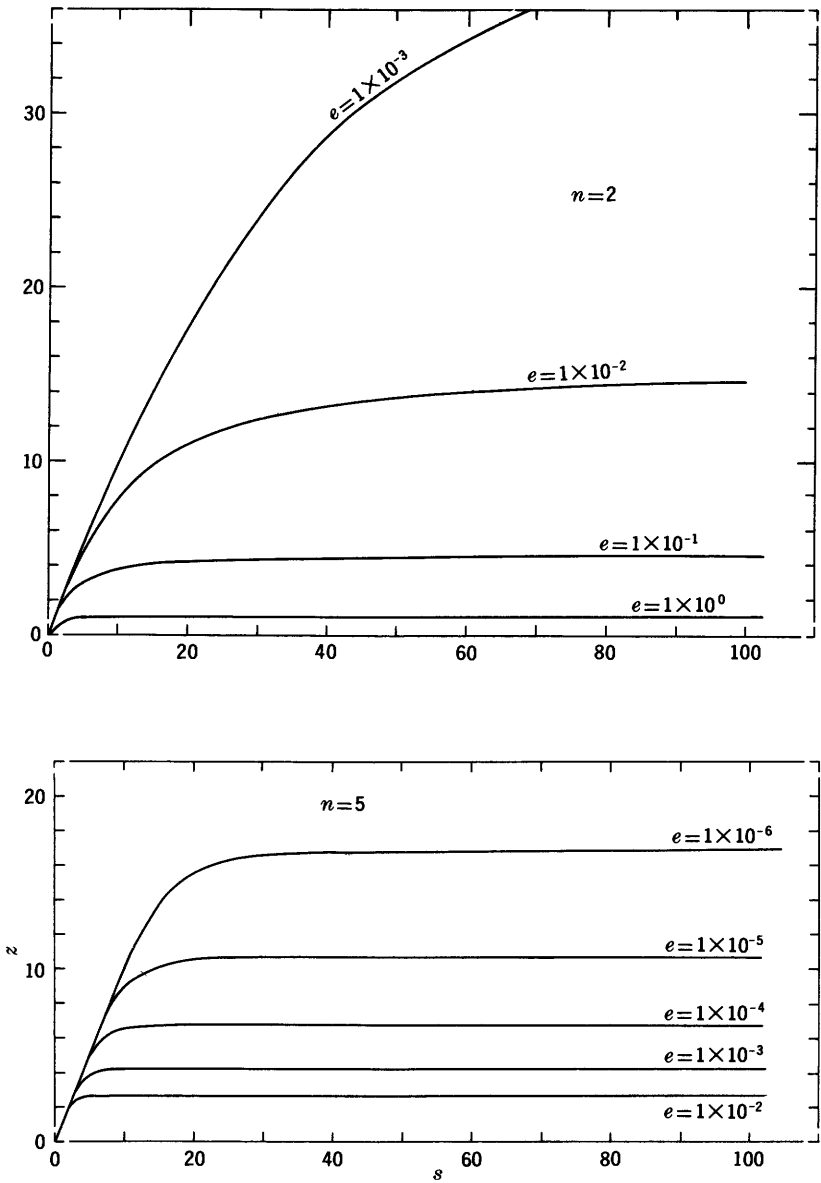
FIGURE 4.—Dependence of dimensionless soil-water suction, s, on dimensionless soil height, z. The numbers labeling the curves indicate the magnitude of dimensionless evaporation rates, e. *Upper*, Soil parameter $n = 2$. *Lower*, Soil parameter $n = 5$.

conditions. This figure demonstrates that for a particular soil and meteorological condition, the evaporation rate remains essentially constant and fixed by weather, if the water-table depth does not exceed a certain value. With the water table at greater depths, the evaporative flux decreases markedly because the soil becomes the limiting factor. In other words,
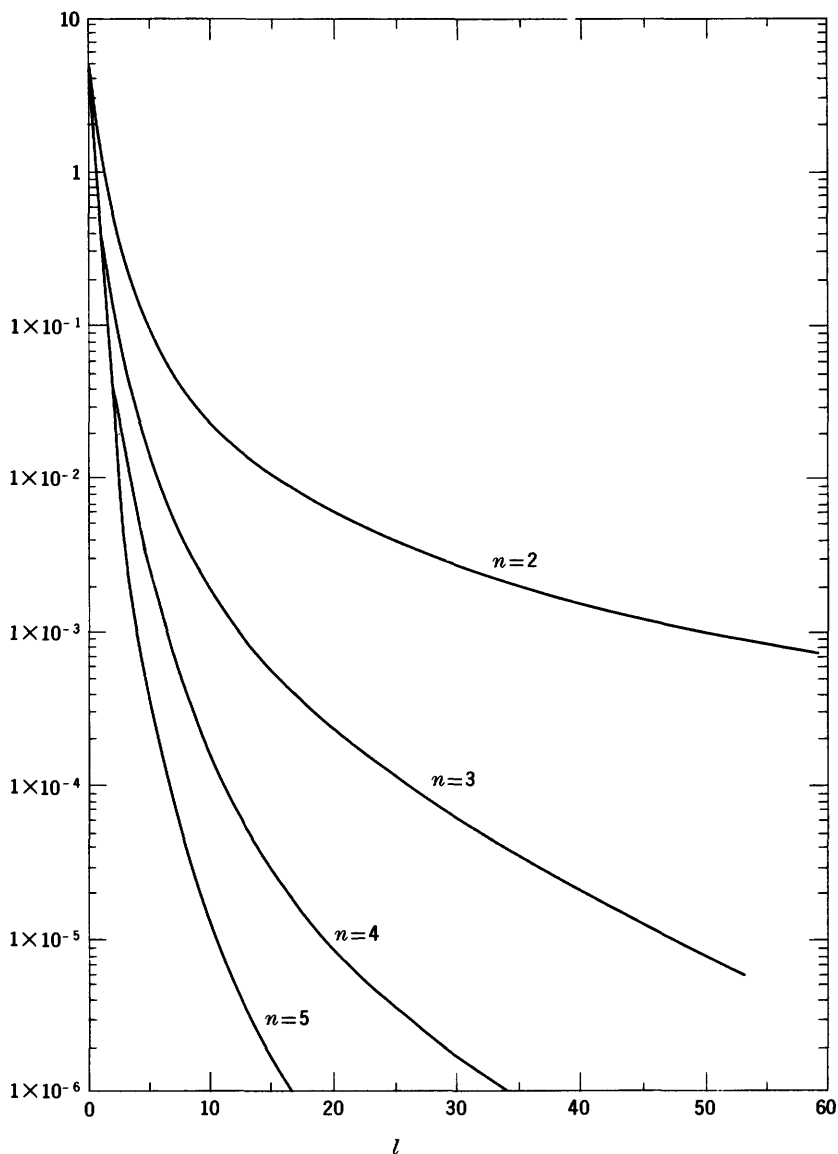
FIGURE 5.—Plots relating dimensionless evaporation, e, to dimensionless depth to water table, l, for $n = 2, 3, 4, 5$.

the flux decreases, because in figure 6 the pertinent meteorological curve intercepts the flat portion of the relevant soil curve. For any given set of meteorological and soil conditions, the transition between the horizontal and descending portions of an appropriate curve in figure 7 is so sharp
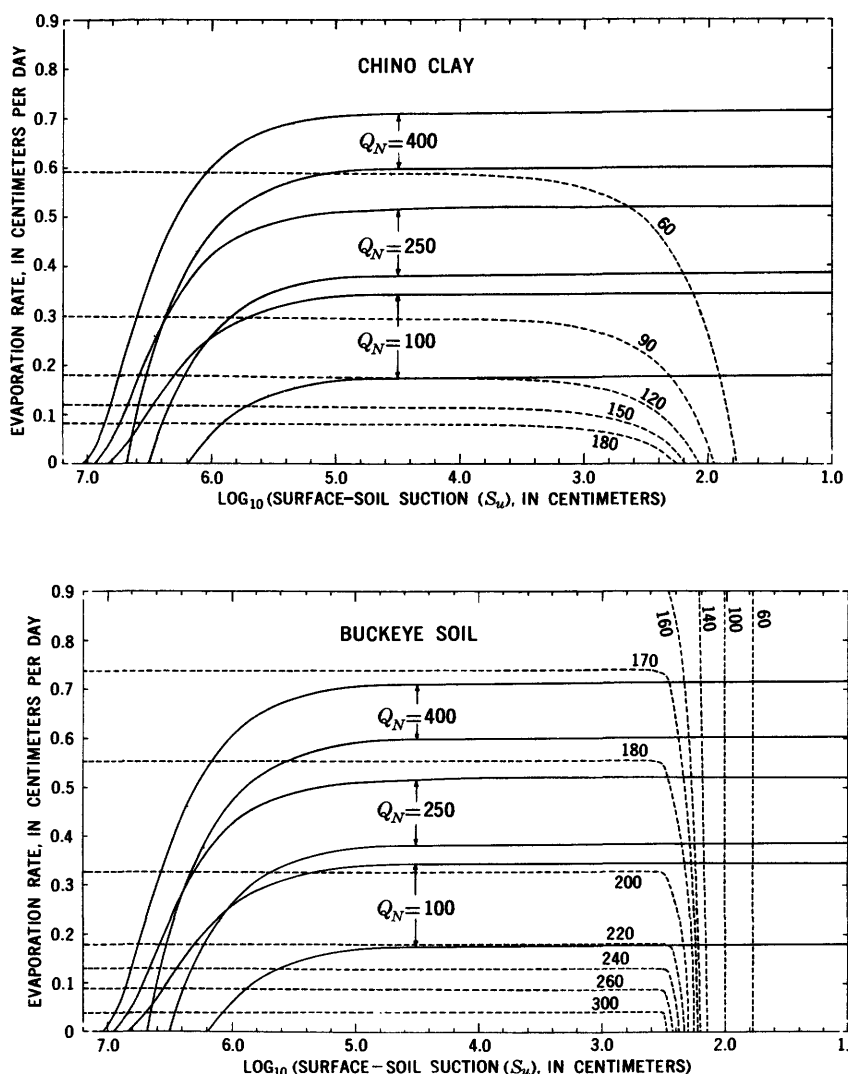
FIGURE 6.—Intercept method for determining evaporation rates, shown for Chino clay and Buckeye soil. The solid lines represent the meteorological curves for wind speed of 6 kilometers per hour, air temperature of 25°C, and for the indicated Q_N values. The top and bottom curves, corresponding to a given Q_N, represent air relative humidities, h_a, equal to 0.02 and 0.75, respectively. The dashed lines represent the soil curves for the indicated water-table depths, L.

that it can be taken as discontinuous, and its curvature can thus be neglected; this fact is in agreement with the observations by Philip (1957b). Therefore, each curve of figure 7 consists essentially of a horizontal part fixed by the weather and a descending part fixed by equation 23 or 24 (that is, by fig. 5).

This characteristic form of the curve leads to the simplicity of the following procedure for determining the actual E. The appropriate soil-limited evaporation, E_∞, may be determined with equation 23 or 24 and plotted against depth to the water table. The appropriate meteorologically controlled potential evaporation, E_{pot}, may then be entered as a straight horizontal line. The actual evaporation for any given water-table depth may be taken as the lowermost portions of the two intersecting curves.

Note that if $E \ll K_{sat}$, as in figure 7, Buckeye soil, the exact and approximate E_∞ curves essentially coincide. Hence, equations 25 or 26 may be used for estimating E under such circumstances. On the other hand, in
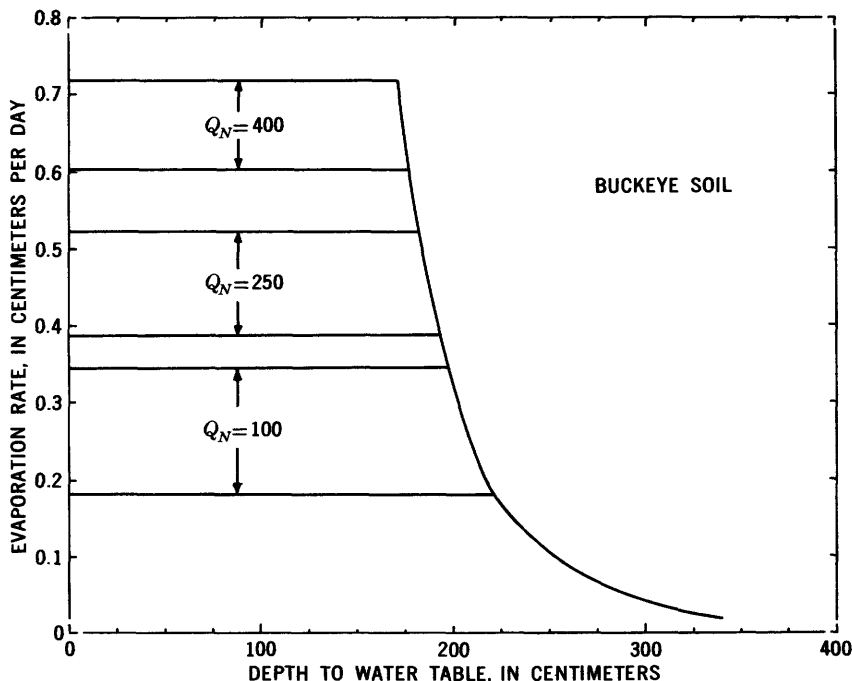
FIGURE 7.—Relation between evaporation rates and water-table depths, shown for Chino clay and Buckeye soil, calculated by the intercept method (solid line). The indicated meteorological conditions are identical with those of figure 6. The descending solid line also represents the exact soil-limited rates of evaporation obtained from equation 23. The dashed line represents the approximate soil-limited rates of evaporation and is obtained from equation 25. The exact and approximate curves coincide in Buckeye soil. Figure 7 continued on next page.
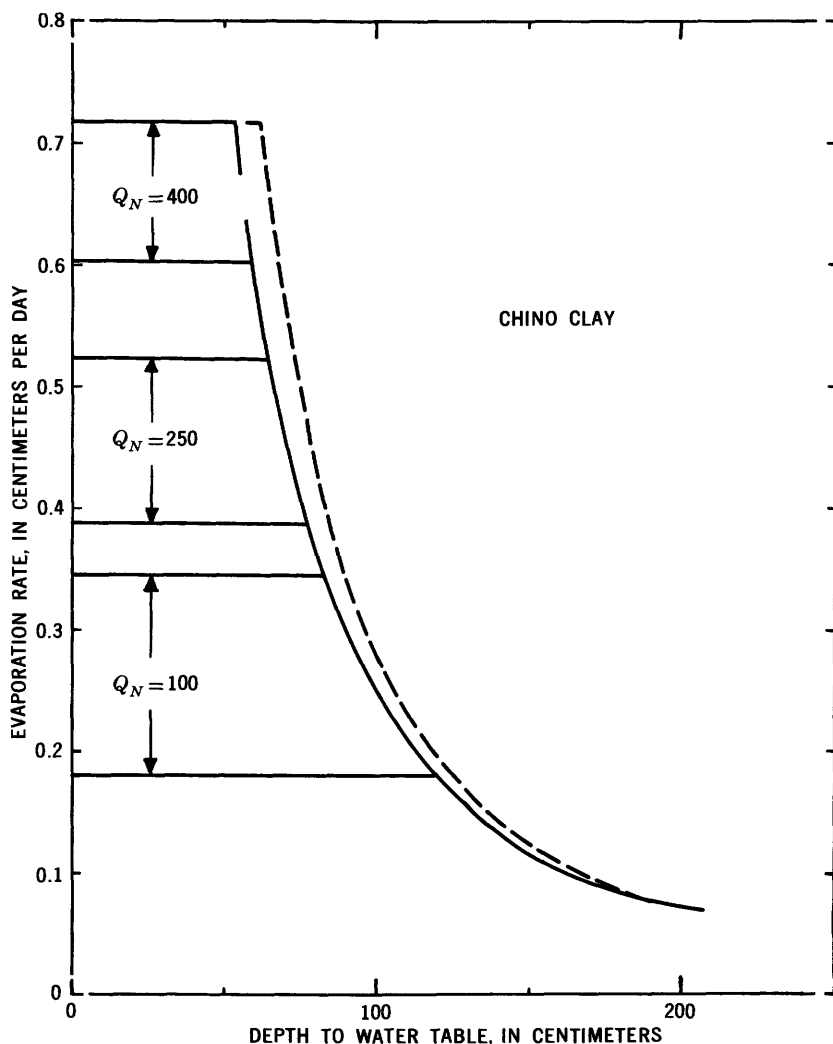
FIGURE 7.—Continued

figure 7, Chino soil, such a coincidence does not occur. As a result, the approximate E_∞ curve overestimates the actual E in the descending portion of the E curve.

Figure 8 illustrates for several water-table depths in Chino soil how efficiently the atmosphere can remove soil water under various meteorological conditions. The index of the meteorological conditions is the potential (that is, $S_u = 0$) evaporation, E_{pot}. The efficiency of removal is measured by the ratio E/E_{pot}. For a given water-table depth, the figure demonstrates that the maximum efficiency of water removal ($=1.0$)
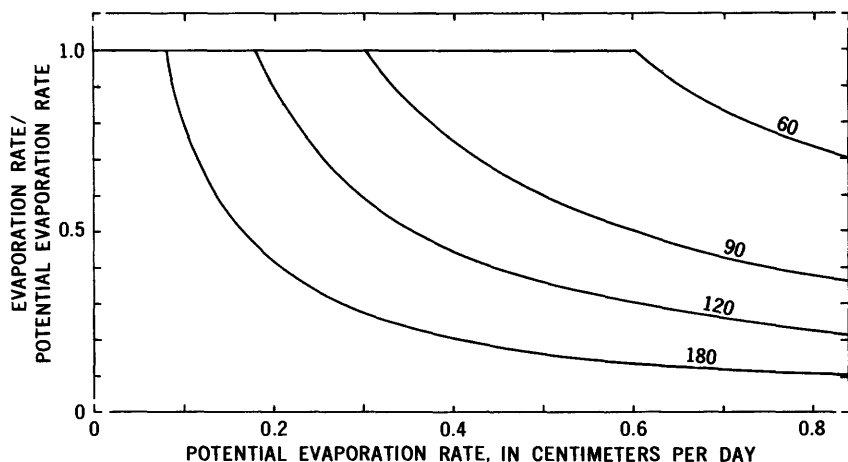
FIGURE 8.—Dependence of relative evaporation rates, $E/E_{\rm pot}$, upon the potential evaporation rates, $E_{\rm pot}$, for Chino clay. Numbers labeling the curves indicate the depths to water table.

occurs at small values of $E_{\rm pot}$. For any given water-table depth, as $E_{\rm pot}$ increases, the efficiency remains at a maximum until a certain limiting $E_{\rm pot}$ is reached; thereupon, the efficiency declines rapidly. This transition point is fixed by the water-table depth and occurs when the evaporation rate becomes limited by the soil's inability to conduct water rapidly enough.

LAYERED SOIL

Steady-state evaporation in a layered system unaffected by vapor transfer may be described by the functional relations appropriate to each layer in a manner analogous to the homogeneous case. For a soil with i layers above the water table (fig. 1, case B), these relations may be symbolized as follows:

Soil layer 1 (lowermost) $L_1 = F_{g_1}(S_1, E)$,   (28–1)

Soil layer 2 $L_2 = F_{g_2}(S_1, S_2, E)$,   (28–2)

Soil layer 3 $L_3 = F_{g_3}(S_2, S_3, E)$,   (28–3)

***   ***   ***

Soil layer i (uppermost) $L_u = F_{g_i}(S_{i-1}, S_u, E)$,   (28–$i$)

The atmosphere $E = F_m(S_u)$.   (29)

In any one of the equations 28–j above (in which the value of j is 1, 2, 3, or i), S_{j-1} and S_j are, respectively, the suctions at the lower and upper interface of layer j. Note that S_0 is known ($S_0 = 0$); therefore, it

does not appear in equation 28–1. Also, in conformance with the earlier symbolism, S_i is designated as S_u. (See equation 28–i.) Presently, the subscript j will also be used for subscripting the coefficients n, $S_{1/2}$, and K_{sat} of the layer j.

The above set of equations may be solved simultaneously since it contains as many equations as unknowns. Such a solution may be achieved using either a numerical or graphical (intercept) method. The latter method will be described presently. Note that, as in the homogeneous case, the present approach is possible owing to the fact that two adjacent layers exhibit identical suctions at their common interface.

It will be recalled that the intercept method discussed previously involves finding the intersection between plots representing the meteorological and soil equations. In applying the intercept method to the layered case, one must deal with sets of parameters which differ from layer to layer. Hence, E and S should be plotted rather than their dimensionless counterparts, although e may be employed in certain computations involving single layers.

The meteorological curve needed is plotted with the aid of equations 4, 5, 6 and 9, as it was in the homogeneous soil case. The graph of the soil equation involves S_u (in addition to E), that is the surface suction of the uppermost layer. To plot such a graph for a layered soil system, a procedure for obtaining S_u from any given E must be used. This procedure involves the determination, for a given E value, of the suction, S_j, at the upper surface of each successive soil layer, starting with $j = 1$ and ending with the appropriate value of S_u for $j = i$.

The equation for computing such a suction at the lowermost layer 1 (fig. 1, case B) is

$$(e_1+1) \left(\frac{e_1}{e_1+1} \right)^{1/n_1} \frac{L_1}{(S_{1/2})_1} = \int_0^{y_1} \frac{dy}{y^{n_1}+1} , \qquad (30)$$

where

$$e_1 = E/(K_{sat})_1$$

and

$$y_1 = \frac{S_1}{(S_{1/2})_1} \left(\frac{e_1}{e_1+1} \right)^{1/n_1} .$$

Note that equation 30 is identical with equation 18 because of the physical similarity of the respective situations. The graphical procedure for obtaining S_1 (utilizing figs. 2 and 3) described for equation 18 is applicable here.

In the second step, the equation used for the relations in layer 2 is

$$(e_2+1) \left(\frac{e_2}{e_2+1} \right)^{1/n_2} \frac{L_2}{(S_{1/2})_2} = \int_{\bar{y}_1}^{y_2} \frac{dy}{y^{n_2}+1} , \qquad (31)$$

where

$$e_2 = E/(K_{sat})_2,$$

$$y_2 = \frac{S_2}{(S_{1/2})_2}\left(\frac{e_2}{e_2+1}\right)^{1/n_2},$$

$$\tilde{y}_1 = \frac{S_1}{(S_{1/2})_2}\left(\frac{e_2}{e_2+1}\right)^{1/n_2},$$

and

$$(\tilde{y}_1 \neq y_1).$$

The derivation of the above equation is identical in principle with that of equation 17; however, the lower boundary condition here is $S = S_1$ and not zero, as it was in equation 17.

Equation 31, for ease in handling, is rearranged as

$$(e_2+1)\left(\frac{e_2}{e_2+1}\right)^{1/n_2}\frac{L_2}{(S_{1/2})_2} + \int_0^{\tilde{y}_1}\frac{dy}{y^{n_2}+1} = \int_0^{y_2}\frac{dy}{y^{n_2}+1}. \qquad (32)$$

With the aid of equation 32 one can find S_2 for the given S_1 and E values. To accomplish this, first compute $\tilde{y}_1$ and e_2, using the relevant definitions given in connection with equation 31. The integral on the left-hand side of equation 32, $I(\tilde{y}_1)$, is then evaluated employing the appropriate curve of figure 3. Next, a technique identical with that of the homogeneous case (and involving fig. 2) is used to determine the magnitude of the first term of equation 32, $f(e_2)L_2/(S_{1/2})_2$. Addition of the latter term to the previously computed $I(\tilde{y}_1)$ yields the value of $I(y_2)$, from which S_2 is computed using figure 3.

Equations such as equation 32, with subscript 2 replaced by $j=3, 4, ***i$, may be written for each additional soil layer. Thus the calculation procedure may be carried stepwise up the soil profile. The equation for the uppermost layer leading to the S_u values sought is

$$(e_i+1)\left(\frac{e_i}{e_i+1}\right)^{1/n_i}\frac{L_i}{(S_{1/2})_i} + \int_0^{\tilde{y}_{i-1}}\frac{dy}{y^{n_i}+1} = \int_0^{y_u}\frac{dy}{y^{n_i}+1}, \qquad (33)$$

where the definitions of $\tilde{y}_{i-1}$ and y_u are similar to those of analogous terms in equation 31.

Often, the only information sought is the dependence of the soil-limited evaporation, E_∞, upon the water-table depth. Such information may be obtained for multilayered systems without determining the individual soil curve and without using graphical or numerical means. Most of the required procedure consists of computing, for various E values of interest, the suctions at the lower surfaces of successive soil layers, starting with the uppermost layer, i, and finishing with the layer

just above the one in which the water table can be found. These computations are followed by calculation of the water-table position in the lowest soil layer, 1.

The equation for the uppermost layer required by such a procedure is derived from equation 33, by noting that e_∞ is associated with an infinite S_u and hence with an infinite y_u. This in turn implies that the integral on the right of equation 33 is equal to $\pi/[n_i \sin (\pi/n_i)]$. (See the derivation of equation 23.) By using this fact, the rearranged equation for the uppermost layer is

$$\frac{\pi}{n_u \sin \left(\dfrac{\pi}{n_u}\right)} - (e_u+1) \left(\frac{e_u}{e_u+1}\right)^{1/n_u} \frac{L_u}{(S_{1/2})_u} = \int_0^{\tilde{y}_{u-1}} \frac{dy}{y^{n_u}+1} . \qquad (34)$$

The value of the left-hand side of equation 34 can be computed for the known parameters involved. From this value, $\tilde{y}_{u-1}$ is determined with the aid of figure 3. The definition of $\tilde{y}_{u-1}$ provides the means of calculating the corresponding S_{i-1}.

The underlying layers, $j = i-1, i-2, ***, 2$, are described by equations identical in form with equation 32, but index 2 is replaced by indices appropriate to the particular layer. These equations may be successively solved for S_{j-1}, progressing downwards, in the manner closely resembling the one described in the preceding paragraph. In each step, the suction previously determined at the lower interface provides the suction value for the upper interface of the analyzed layer. This procedure may be carried out stepwise, down the soil profile, for any number of discrete soil layers, until the lowermost layer is reached. At this point, equation 30 is used with y_1 known from the solution of the equation appropriate to the layer just above. This equation is applicable because the suction at the lower surface of layer 1 (the water-table surface) is equal to zero for all cases. Equation 30 may be used for determining the value of L_1 that corresponds to the value of E employed. The final result of such a computation for a given value of E is the relevant depth to the water table expressed as the sum total of soil-layer thicknesses. Note that as computations for various E values progress, the water-table position may be found to shift from one soil layer to an adjacent one. Such cases would necessitate an appropriate adjustment in the computation procedure outlined above.

Figure 9 demonstrates the application of either of the above two computation methods to Buckeye soil with (1) no crust, (2) the same soil overlain by a slightly salt-cemented upper crust ($n=4$, $S_{1/2}=28.1$, $K_{sat}=47$) of either 3- or 10-cm thickness, and (3) the same soil overlain by the 10-cm crust of the previous layer plus an uppermost 10-cm layer of a hypothetical soil ($n=3$, $S_{1/2}=20$, $K_{sat}=20$). The figure shows clearly
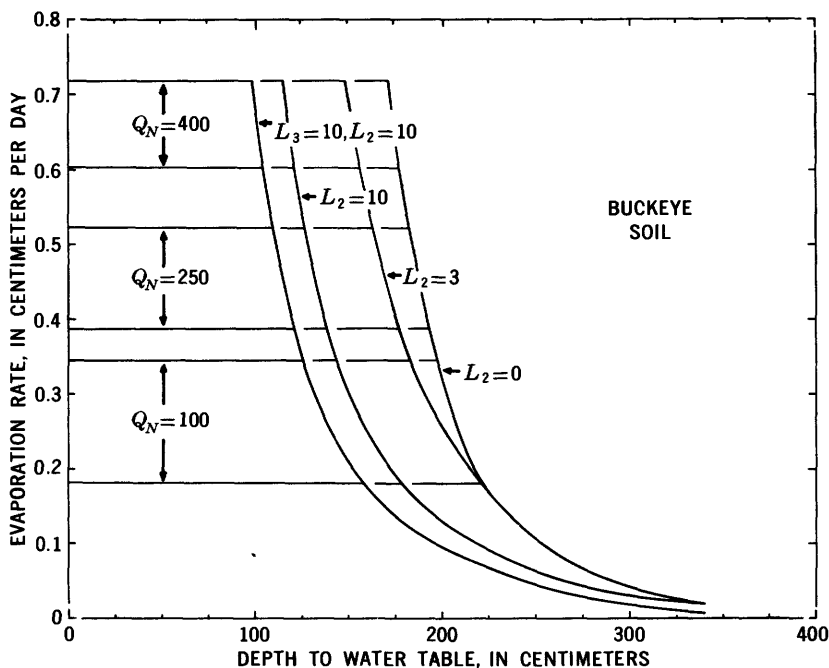
FIGURE 9.—Influence of layering on the relation between evaporation rate and depth to water table. Limiting curves of soil-water evaporation are shown for the homogeneous case ($L_2=0$), a two-layered soil, with the upper layer thickness, L_2, of either 3 or 10 cm, and a three-layered soil with the thickness of intermediate and uppermost layers equal to $L_2=10$ cm and $L_3=10$ cm, respectively.

that a relatively thin less permeable layer may markedly decrease evaporation rates.

EFFECTS OF VAPOR TRANSFER

If a homogeneous soil in contact with a water table is sufficiently dry near the surface, water transfer in the dessicated, upper region involves primarily vapor rather than liquid flow. Vapor flux in this layer may depend significantly on soil-temperature gradients. The probable existence of such a transfer can be detected by noting that, in general, appreciable vapor-transfer influences in soils tend to occur when $h \leq 0.8$ (Philip and de Vries, 1957; Rose, 1963b; Jackson, 1964). To utilize this fact, derive h_u, by using the previously described procedures for cases unaffected by vapor transfer (for example, after computing E, employ equation 5 to evaluate h_u). If the derived h_u value is smaller than 0.8, E might be significantly affected by vapor transfer.

When the dessicated, upper layer in question is present, a more or less exact evaluation of E involves numerical integrations and is based on

heat-transfer as well as water-transfer equations. The approach outlined below avoids this relatively complex procedure, but it is clearly approximate. This approach utilizes a suggestion originally made by Gardner (1958) and a theory of vapor transfer in soils developed by Philip and de Vries (1957). (See also de Vries, 1958.)

Gardner suggested that the homogeneous soil-water system in question may be represented approximately by a two-layered column (fig. 1, case C) in which water is being transported exclusively in vapor form within the upper layer u, while in the lower layer 1 only liquid flow takes place. The theory of Philip and de Vries (1957) applied to the dry, upper soil layer of such a system may be formulated in terms of humidity and temperature gradients. Such a formulation results in the following equation of vapor flow:

$$E = -D_{hv}\frac{dh}{dz} - D_{Tv}\frac{dT}{dz} \qquad (35)$$

where

$D_{hv}=$ a coefficient characterizing the molecular diffusion of soil-water vapor caused by humidity gradients, cm^2 day^{-1}, and

$D_{Tv}=$ a coefficient characterizing the molecular diffusion of soil-water vapor caused by thermal gradients, cm^2 day^{-1} °K^{-1}.

It can be shown (Penman, 1940; Philip and de Vries, 1957) that the coefficient D_{hv} is described by

$$D_{hv} = D_a\Phi(\sigma)\{P/[P-hp(T)]\}\rho_v(T)/\rho_w, \qquad (36)$$

where

D_a = a coefficient characterizing the molecular diffusion of water vapor in free air, cm^2 day$^{-1} = 50.91T^{2.3}/P$, (de Vries, 1958),

P = ambient pressure, mb,

σ = volumetric air content of the soil, dimensionless,

$\Phi(\sigma)=$ a dimensionless function defining the effectiveness of the water-free pore space for diffusion, $\cong \alpha\sigma$,

α = tortuosity factor, dimensionless$\cong 0.66$, and

ρ_v = $\rho_v(T)=$ density of saturated water vapor, gm cm^{-3}; ρ_v is a function of temperature.

According to the Philip and de Vries theory, the coefficient D_{Tv} is given by

$$D_{Tv} = D_a\eta\{P/[P-hp(T)]\}(d\rho_v/dT)\zeta h/\rho_w, \qquad (37)$$

where

$\eta=$ soil porosity, dimensionless, and

$\zeta=$ a ratio of the average temperature gradient in the air-filled soil

pores to the overall soil temperature gradient; this ratio depends upon soil porosity, water content, temperature, and quartz content, and it usually varies between 1.3 and 2.3, except in extremely dry, compact soils in which it may reach the value of 3.2, especially if the soil contains much quartz. (See Philip and de Vries, 1957; Rose, 1968.)

Note that

$$D_{Tv} = BhD_{hv}, \qquad (38)$$

where

$B = (\eta/\sigma)(\zeta/\alpha)[d(\log_e \rho_v)/dT] = (\eta/\sigma)(\zeta/\alpha)\beta'$, gm cm^{-3} °K^{-1}, and

$\beta' = d(\log_e \rho_v)/dT \cong 0.1516 - 3.22 \times 10^{-4}T$; the latter empirical equation has been fitted for 290°K $< T <$ 360°K by using data from List (1951).

It follows from the expressions for D_{hv} and D_{Tv} given above that equation 35 can be written

$$-\frac{E}{D_{hv}} = \frac{dh}{dz} + Bh\frac{dT}{dz}. \qquad (39)$$

Utilization of equation 39 is facilitated by the following approximations, which are made possible by the low water content of the upper soil layer in question. First, in dry soils, the volumetric air content, σ, is approximately constant and equal either to porosity, η, less the water content of air-dry soil, or to η alone, if the water content is negligible. Hence the ratio η/σ of B is approximately constant and often equal to unity. It may be noted that of the other factors determining B, only ζ depends on variables other than temperature. In this study, the ratio ζ, which in all soils is generally of the same order of magnitude, will be taken as a constant, and all the computations needed for determining E will be carried out twice: once for the probable minimum value of ζ ($\zeta \cong 1.3$) and another time for the corresponding maximum value ($\zeta \cong 2.3$). It can be shown that such calculations lead to the estimation of the probable upper and lower bounds of the E value sought. The above considerations indicate that in this study it will be possible to regard B as determined by temperature alone. Second, in dry soils, the ratio $P/[P-hp(T)]$ is approximately equal to unity. Hence, the coefficient D_{hv} of equation 39 can be regarded as a function of temperature alone.

In addition to the above approximations and to soil and meteorological data, which are needed in the previously discussed cases, the approach under consideration requires two new assumptions, as well as information about soil temperature, T_1, at one small depth, L_u^*. This depth is defined here as one which may exhibit a significant gradient of the mean daily

temperature. In the computations of this study, the L_u* value was taken as 2 cm.

The first new assumption required is that the temperature gradient in the dessicated, upper layer (of depth L_u) does not vary with layer thickness and is approximately equal to $(T_u - T_1)/L_u*$.

The second new premise is based on the fact that D_{hv} and B, though temperature dependent, do not vary greatly with T. Owing to this, the following can be assumed for temperature ranges commonly met near the soil surface: D_{hv} and B are independent of temperature, if they are evaluated at the mean temperature of the upper soil layer defined as $\frac{1}{2}(T_u + T_1)$.

The above two premises tend to imply that the depth of the upper layer in question, L_u, is not very different from L_u*. If the procedure to be derived presently yields results which are strongly at variance with this implied assumption, a satisfactory assessment of E may require certain special measures. These will be described in due course.

With the aid of the above approximations and premises, equation 39 can be easily integrated. First, this equation is rewritten in a slightly different form,

$$\frac{dh}{dz} = b\left(h - \frac{c}{b}\right), \tag{40}$$

where

$$b = -B(T_u - T_1)/L_u*$$

and

$$c = E/D_{hv}.$$

Second, h of equation 40 is replaced by a new variable, φ, defined by $\varphi = h - (c/b)$. The resulting equation in φ is readily solved by separation of variables, using boundary conditions, which state that the variable h assumes the values of h_1 and h_u at $Z = (L - L_u)$ and $Z = L$, respectively. This solution yields, after rearrangement, the working equation of the procedure under consideration,

$$L_u = \frac{2.3}{b} \log_{10} \frac{h_u - (c/b)}{h_1 - (c/b)}. \tag{41}$$

Equation 41 makes it possible to compute L_u for a given E, if the relevant soil properties are known and if the given value of E is plausible under the assumptions made. Note that because of the latter limitation, when b is positive (that is, when $T_u < T_1$), there will exist certain arbitrarily chosen E values for which equation 41 cannot yield a meaningful answer.

The value of h_1 in equation 41 may be taken as corresponding to the soil-moisture suction at which the vapor-transfer influences become

sufficiently important. According to theoretical considerations of Philip and de Vries (1957) and measurements by Rose (1963b), liquid flow commences at $h \cong 0.6$. Jackson's (1964) experiments suggest for desorption that this value may lie between 0.5 and 0.8. The commencement of appreciable vapor-transfer influences probably occurs at somewhat higher values of h than those associated with the commencement of liquid flow. Hence, perhaps h_1 could be taken as at least equal to 0.8. For a given soil, the soundness of this choice can be checked and possibly improved by comparing the value of $K = K_{1iq}$ at $h = 0.8$ (computed with the aid of equations 6 and 10) and the value of the corresponding coefficient of isothermal vapor transfer (Rose, 1963a), $K_{vap} = (MghD_{hv})/(RT)$. If $K_{vap} \cong K_{1iq}$, it is very probable that the value of h_1 chosen was suitable.

Whichever reasonable value of h_1 is used, the interface suction S_1, which corresponds to h_1, is relatively high and usually exceeds 10,000 cm. For suctions of this magnitude the rate of water flow in the moist soil below the interface in question is essentially soil limited. Hence, the rate of water transfer in the lower, moist soil layer can be evaluated with the aid of equation 23. If the thickness of the moist layer is taken as $L_1 = L - L_u$, then for steady-state conditions and any given L, equation 23 (with its L replaced by $L - L_u$) in effect expresses E as an increasing function of the dry-layer depth, L_u.

Another relation, giving E as a decreasing function of L_u, is expressed by the just-derived equation 41. The two equations linking E and L_u (equations 23 and 41) can be solved simultaneously, either graphically or numerically, to yield the actual E and L_u.

If the value of L_u thus obtained is of a different order of magnitude than $L_u{}^*$, the actual E which corresponds to L_u should be reassessed. If $L_u \ll L_u{}^*$, it might be desirable to acquire new T_1 data for an appropriately small $L_u{}^*$ and to repeat the original procedure, using the new T_1. On the other hand, if $L_u \gg L_u{}^*$, it is advisable to consider the upper layer, u, as consisting of two sublayers. In the upper sublayer, nonisothermal vapor transfer can be taken as the predominant manner of water transfer; equation 41 describes the relevant relations for such a region. If the depth of this sublayer is assumed to be $L_u{}^*$ and if E is given, humidity, $h_1{}^*$, at the bottom of the sublayer in question can be computed, since it follows from equation 41 that

$$h_1{}^* = (c/b) + [h_u - (c/b)]/\exp(-bL_u{}^*). \qquad (42)$$

In the lower part of layer u, isothermal vapor transfer can be assumed to be the dominant mode of water flow. Such a flow is described by equation 35, with $dT/dz = 0$. Integration of this equation, leads to the relation

$$L_u{}' = (h_1 - h_1{}^*)/(E/D_{hv}) \qquad (43)$$

in which $L_u{}'$ is the depth of the lower sublayer.

For a given E, the reassessment procedure just outlined can produce a corresponding value of $L_u (= L'_u + L^*_u)$. Thus, a relation between E and L_u can be obtained for a set of arbitrarily selected E values. As in the first vapor-case procedure described above, such a relation can be used in conjunction with equation 23 to determine, either graphically or numerically, the desired values of the actual E and L_u.

The above procedures for including vapor transfer in the evaporation computations were tried out with the data of the Buckeye soil on hand and with several estimated T_1 values. The results obtained showed that under the conditions tested $(T_u > T_1)$, the E value was somewhat increased by the vapor-transfer influences. This increase, however, did not exceed 0.01 cm per day (less than 5 percent of E) and hence could be neglected for most practical purposes. (Compare with the results of Hanks and Gardner, 1965.) The reason for so slight an increase probably is twofold. Firstly, the values of D_{hv} and D_{Tv} are rather small. Secondly, when $T_u > T_1$, thermal transfer is counteracting the influence of the humidity gradients. If, however, conditions are such that significant vapor-transfer effects are suspected, the methods given in this section can be used to estimate such influences.

DISCUSSION, EXPERIMENTAL TEST, AND CONCLUSIONS

Of the relations which can be computed with the aid of the approach presented in the preceding pages, the one which might be most useful in hydrologic practice is described by the plots of E versus L, as those in figures 7 and 9. A summary of the procedure based on using these plots is given in the flow chart at the end of this report. The results obtained in this study confirm Philip's (1957b) contention that for all practical purposes, plots of this kind can be prepared by assuming that for any given L, the actual $E(L)$ is the smaller of E_{pot} and $E_\infty(L)$. In such cases, the latter two quantities may be calculated, respectively, with the aid of the appropriate meteorological and soil equations. It follows that the actual E is either atmosphere limited or soil limited. This implies that the region on the $E(L)$ plots in which both atmospheric and soil factors are influential is so small that it can be neglected. For a Yolo light clay, Philip noted that the impreciseness due to such a neglect as compared with the exact solution was smaller than could be exhibited on a graph of the scale he used. The experience of this study, in which two very different soils were used, was similar.

The reason for the narrowness of this region of imprecision is suggested by the shape of the curves shown in figure 6. An inspection of these curves reveals that the S_u axis may be divided into the following three regions: (1) a low suction region (roughly $S_u < 6 \times 10^3$) in which the soil curves may show relatively steep slopes but in which the meteorological curves are nearly horizontal and are fixed by $E \cong E_{pot}$, (2) an intermediate suction

region (approximately, $6 \times 10^3 < S_u < 6 \times 10^4$) in which soil and meteoro­logical curves are nearly horizontal and approach their respective, limiting E values, and (3) a high suction region $(S_u > 6 \times 10^4)$ in which the meteorological curves exhibit appreciable slopes, whereas the soil curves are practically horizontal and are fixed by $E \cong E_\infty$. From the above it is clear that an intersection between meteorological and soil curves which occurs in the low-suction range results in $E \cong E_{pot}$. On the other hand, when such an intersection occurs on the high-suction range, one obtains $E \cong E_\infty$. The intersections which occur in the intermediate range involve plots with nearly horizontal slopes of opposite sign. Hence, for any given set of weather and soil parameters only a limited range of water-table depths will produce intersection values confined to the intermediate S_u range. In this range the values of E may vary somewhat; however, the almost horizontal character of the curves specifies that the actual value of E lies between the very nearly equal values of E_{pot} and E_∞. Therefore, for all practical purposes, $E \cong E_{pot} \cong E_\infty$ for the intermediate range. It follows from the above considerations that in all three suction ranges, the actual E must be almost equal either to E_∞ or to E_{pot} or to both of these quantities.

The conclusion just stated very probably is not restricted to the soil and weather conditions treated in the examples of this study, and it can be expected to be applicable rather generally. The reasons for this are as follows. Equation 3 demonstrates that the meteorologically determined E is a linear function of h_u; however, it follows from equation 6 that $h_u = \exp\left[(-MgS_u)/(RT_u)\right] = \exp\left[\mu^2 \times 10^{-7} S_u\right]$ where $\mu^2 < 8$ for the commonly found surface-soil temperatures, T_u. Hence, h_u deviates appreciably from 1.0 (that is, from full saturation) only if the S_u value is very high. This accounts for the fact that the meteorological curve deviates from the horizontal only in the high S_u range. On the other hand, it follows from equation 22 and figure 3 that for the usual soil parameters and evaporation rates, the soil curves almost reach their limiting level when S_u is still relatively low. This accounts for the soil-curve contribution to the peculiarities of the $E(L)$ relation under consideration.

An inspection of figure 6 indicates that in the intermediate suction range, the $E(S_u)$ curves drawn for soils with low-valued n parameters (for example, $n = 2$) show the largest slopes, whereas the soils with large n values (for example, $n = 5$) exhibit the smallest slopes. Also, this conclusion is implied by the curves of figure 3. It follows from such a conclusion that in the intermediate suction zone, the lower the value of n, the larger the limited range of transitional E values which depend on both soil and meteorological factors. This might suggest that the $E(L)$ estimation procedure under consideration is least precise with soils of low n values. Even in these cases, however, the procedure was found sufficiently accurate for most practical purposes. Note also that the

appreciably sloping parts of the soil and meteorological curves shift towards the intermediate suction region as the limiting E values decrease. Hence, the relative importance of the transitional E range increases as the magnitude of the limiting E decreases. But for these small values of E, the absolute importance of any imprecision of E in the intermediate suction range is insignificant.

To test in a preliminary way the applicability of the $E(L)$ estimation procedure considered above, its results were compared with actual field observations. The field data were obtained from two large bare-soil evaporation tanks located at Buckeye, Ariz., and described by van Hylckama (1966). The local soil contained in these tanks had a slightly salt-cemented upper layer (layer 2 discussed above in the layered-soil case) that appeared to be somewhat thicker than 10 cm.

The tanks were provided with apparatus for automatically maintaining a preselected water-table depth and for recording the quantity of water required to do this. Consequently, data on the actual daily rate of evaporation for a selected depth to water table was readily obtained.

Meteorological data, which included air temperatures, air relative humidities, and wind velocities, were also collected hourly at the site. These variables, converted to a daily-average basis, along with tabular radiation data appropriate to the site (List, 1951), were used to calculate E_{pot} by the methods described earlier in this paper. Also, soil temperatures at the depths of 5 and 10 cm were recorded.

Data sets of various periods were chosen for analysis, primarily on the basis of completeness of both actual E and E_{pot} information and achievement of a steady state. All these sets were selected from March to October data of 3 consecutive years.

To provide information needed for calculation of E_∞, undisturbed soil cores were obtained from the evaporation tanks at depths of 0–10 cm and 50–60 cm. The cores, 3 cm thick and 5 cm in diameter, were taken in successive, spaced pairs from each depth zone with a soil sampler provided with retainer rings. Using the local ground water of the area, saturated hydraulic conductivities and moisture-retention curves were determined on cores selected from the two layers. Each moisture-retention curve was determined in two parts. A ceramic plate with a hanging water column was utilized for the 0 to 0.1 bar suction range, whereas a pressure-plate apparatus (Richards, 1954, method 32) was used for suctions between 0.1 and 1.0 bar. The moisture-retention curves for the two soil zones were used to compute the appropriate n and $S_{1/2}$ parameters by the methods described earlier in this report. These parameters were then used, along with the K_{sat} data, to calculate E_∞ by the procedure outlined in the section of this paper concerned with layered soil.

A comparison of the observed evaporation rates with calculated E_∞ and E_{pot} is illustrated in figure 10. The circles on the plot indicate average
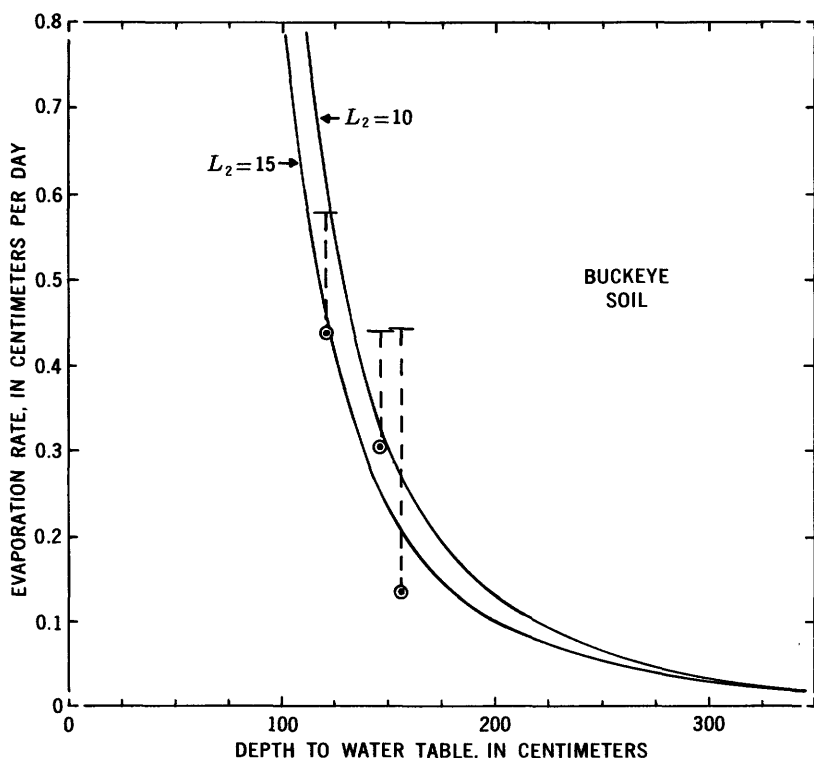
FIGURE 10.—Influence of water-table depth on actual and estimated rates of evaporation from the Buckeye tanks. Computed soil-limited evaporation levels are indicated by the solid lines. The soils involved are two layered, with the upper layer thickness, L_2 centimeters. Each circle and each bar connected with it represent, respectively, an observed mean evaporation rate and the corresponding calculated mean potential evaporation.

observed evaporation rates for three depths to water table. Owing to the insufficiency of the available data, these averages do not carry the same weight. The circles, indicating the 120-, 146-, and 156-cm depths, represent the averages from 55, 13, and 6 days, respectively. The bars connected in figure 10 to the appropriate circles by dotted lines represent the average E_{pot} values calculated from the meteorological data obtained for identical time periods. Also plotted in figure 10 are two E_∞ curves calculated, as mentioned above, for a layered soil. The upper and lower E_∞ curves correspond, respectively, to assumed 10- and 15-cm depths of the cemented, upper soil layers.

Figure 10 shows that under the conditions studied, evaporation was soil limited. Also, this figure demonstrates that the observed values correlate reasonably well with those predicted by the layered-soil esti-

mating technique. Since layered soils are quite prevalent in the field, the method's suitability for handling such situations is an attractive feature.

In spite of these encouraging results it must be stressed that owing to the various premises involved in the derivation of the theoretical meteorological and soil relations of this study, the procedure suggested here is subject to obvious limitations.

Steady-state conditions were assumed throughout this paper. In nature, however, the systems considered are seldom in such a state, principally because of the variations in meteorological conditions, in soil salt content, and in water-table depth.

Owing to the periodicity of the meteorological and water-table changes it might be hoped that use of daily averages for the input data will decrease the errors inherent in a steady-state model applied to transient situations. Gardner and Hillel (1962) suggested that the circadian variation in evaporation rate is effectively damped in the upper few centimeters and that the overall evaporation rate is subject to little error. It is doubtful, however, that such errors are diminished to negligible proportions.

The changes in soil salt content and water-table depth are relatively slow, and therefore their short-period effects might be negligible. Their long-range influences, however, could be of very considerable importance and should be taken into account, perhaps by assuming a series of steady states, with different experimentally determined soil parameters and measured or predicted water-table depths. The effects of salts accumulating and often precipitating in the surface layers might be particularly significant, especially when leaching rains are infrequent and groundwater solute content is relatively high.

Under various conditions, the thermal transfer of water might significantly change the evaporation rate. In this study, such a transfer was taken into account only in the last case treated (that is, the case affected by vapor flowing within the upper, relatively dry soil layer). Thus, the thermal transfer of liquid water was entirely neglected. This approximation seems to be justified because (1) in moist soils such a transfer usually is negligible in comparison with the coexisting liquid flow due to pressure gradients and (2) in dry soils such a transfer is usually insignificant in comparison with the coexisting thermal flow of vapor. (See Philip (1957a) and de Vries (1958) for some typical relative magnitudes of the relevant transfer coefficients.)

The analysis of the vapor-affected case presented in this study attempts to treat the most important of the thermal influences taken into account by the Philip-de Vries theory. It must be stressed, however, that the simple analysis under consideration is based on several assumptions, which are extraneous to the above theory and which can be only approximately valid. These assumptions may influence the vapor-effect correction,

though it is very doubtful that they could change it sufficiently to be of practical significance.

Some of the temperature effects which all the suggested procedures do take into account involve soil surface temperature, T_u. In practice, inaccuracies will exist in data needed to compute the effects of T_u (especially those involved in determining Q_V), and thus the approach used may be imprecise. Also, if a zero value is assumed for Q_g, as was done in this study, the surface temperature, T_u, may be overestimated or underestimated. Information on the thermal conductivity of the soil and soil temperature at a shallow depth could make it possible to account for a nonzero Q_g, but this would necessitate the gathering of additional data with possibly negligible improvement of the overall estimate.

The soil data employed also might be less precise than desirable. This could be at least partly due to the inapplicability of the empirical equation 10 or to the inaccuracy of the methods suggested for deriving hydraulic-conductivity information from the soil-water retention curve. In addition, it might be impossible to take into account adequately the variability of field soils.

Finally, inherent in the method are all the limitations of the basic meteorological and soil equations (equations 3, 4, 9, 10, Darcy's law, and the Philip-de Vries theory).

With the surface-temperature equation 9 included in the computation scheme, the procedure described in this paper might be called quadri-combinational, because it is an algorithm which combines a soil equation of water flow and meteorological equations of heat balance, vapor transfer, and sensible heat transfer. Alternate forms of some of these equations could be employed, and other ways of including them in the algorithm could possibly be devised. The relative merits of such variants of the proposed approach will have to be determined experimentally.

It follows from the above considerations that the technique described in this paper is only approximate and that therefore it should be used with appropriate care. It is possible to devise changes in this technique which would considerably improve its precision; however, these changes would impair the method's relative simplicity and its dependence on generally available data. The preliminary experimental results cited above as well as theoretical considerations seem to indicate that in spite of its limitations, the procedure for evaluating evaporation presented in this paper can yield useful approximate estimates. It should be used primarily when simplicity is needed and precision of estimates is not crucial.
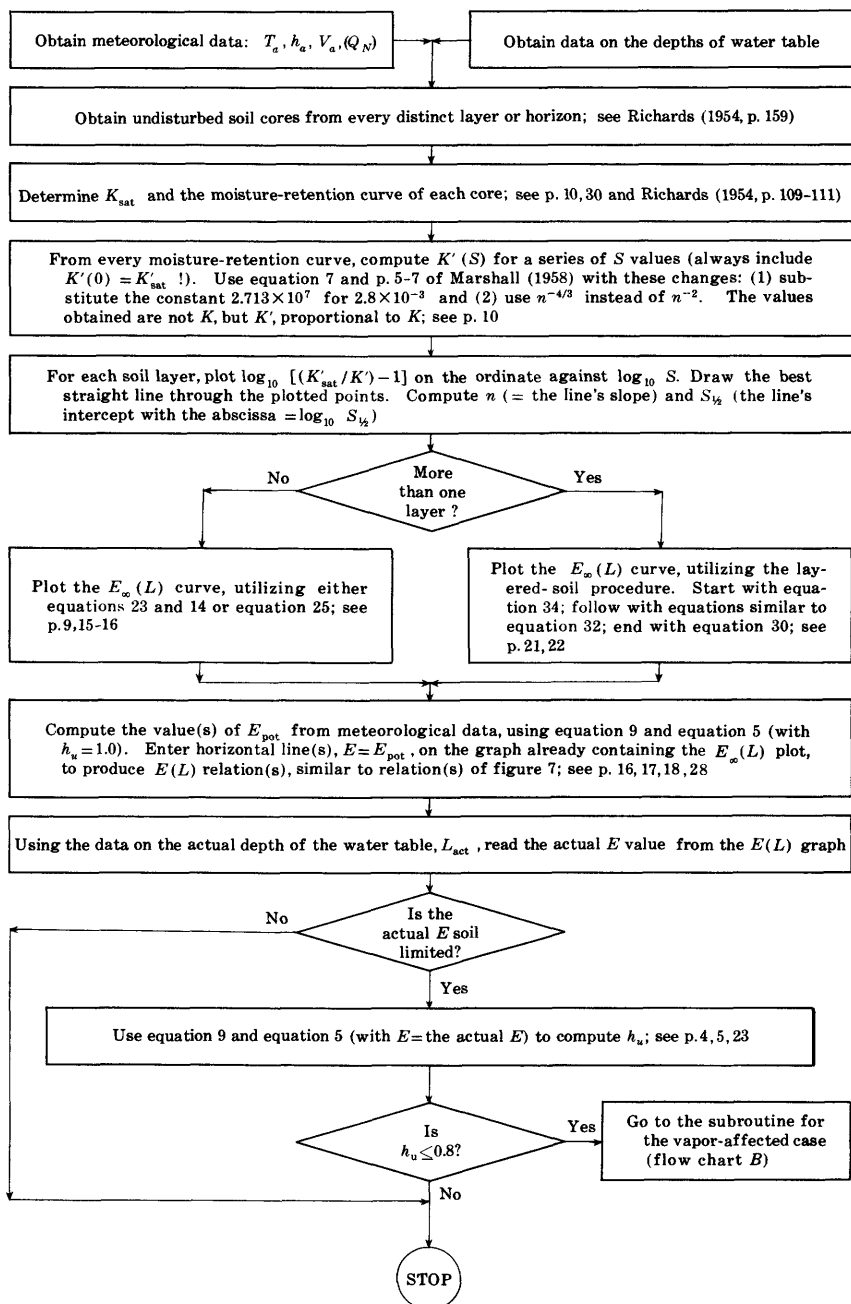
REFERENCES CITED

Arbhabhirama, Anat, Duke, H. R., and Corey, A. T., 1965, Steady upward flow from water tables: Hydrology Paper No. 7, Colorado State Univ., Fort Collins, Colo., 34 p.

de Vries, D. A., 1958, Simultaneous transfer of heat and moisture in porous media: Amer. Geophys. Union Trans., v. 39, p. 909–916.

Edlefson, N. E., and Anderson, A. B. C., 1943, Thermodynamics of soil moisture: Hilgardia, v. 15, p. 31–298.

Gardner, W. R., 1958, Some steady-state solutions of the unsaturated moisture flow equation with application to evaporation from a water table: Soil Sci., v. 85, no. 4, p. 228–232.

———— 1964, Water movement below the root zone: Internat. Soil Sci. Cong., 8th, Bucharest, Rumania, v. 2, p. 63–68.

Gardner, W. R., and Fireman, Milton, 1958, Laboratory studies of evaporation from soil columns in the presence of a water table: Soil Sci., v. 85, no. 5, p. 244–249.

Gardner, W. R., and Hillel, D. I., 1962, The relation of external evaporative conditions to the drying of soils: Jour. Geophys. Research, v. 67, no. 11, p. 4,319–4,325.

Gradshteyn, I. S., and Ryzhik, I. M., 1965, Table of Integrals, Series, and Products [Translated by A. Jeffrey]: New York, Academic Press, 1,086 p.

Hanks, R. J., and Gardner, H. R., 1965, Influence of different diffusivity-water content relations on evaporation of water from soils: Soil Sci. Soc. Amer. Proc., v. 29, no. 5, p. 495–498.

Harbeck, G. E., 1962, A practical field technique for measuring reservoir evaporation utilizing mass-transfer theory: U.S. Geol. Survey Prof. Paper 272–E, p. E101–E105.

Hildebrand, F. B., 1956, Introduction to Numerical Analysis: New York, McGraw Hill Book Co., 511 p.

Jackson, R. D., 1964, Water vapor diffusion in relatively dry soil; Part 2, Steady-state experiment: Soil Sci. Soc. Amer. Proc., v. 28, no. 4, p. 467–470.

Jackson, R. D., Reginato, R. J., and van Bavel, C. H. M., 1965, Comparison of measured and calculated hydraulic conductivities of unsaturated soils: Water Resources Research, v. 1, no. 3, p. 375–380.

List, R. J., 1951, Smithsonian meteorological tables: Smithsonian misc. Colln., v. 114, 527 p.

Marshall, T. J., 1958, The relation between permeability and size distribution of pores: Jour. Soil Sci., v. 9, no. 1, p. 1–8.

Millington, R. J., and Quirk, J. P., 1961, Permeability of porous solids: Faraday Soc. Trans., v. 57, p. 1,200–1,206.

Penman, H. L., 1940, Gas and vapour movements in the soil; Part 1, The diffusion of vapours through porous solids: Jour. Agr. Sci. [Great Britain], v. 30, p. 437–462.

Philip, J. R., 1957a, Evaporation, and moisture and heat fields in the soil: Jour. Meteorology, v. 14, p. 354–366.

———— 1957b, The physical principles of soil water movement during the irrigation cycle: Internat. Comm. Irrig. Drainage Cong., 3d, New Delhi 1957, Trans., v. 3, p. 8.125–8.154.

Philip, J. R., and de Vries, D. A., 1957, Moisture movement in porous material under temperature gradient: Amer. Geophys. Union Trans., v. 38, p. 222–232.

Richards, L. A., (editor), 1954, Diagnosis and improvement of saline and alkali soils: U.S. Dept. Agriculture Handb. 60, 160 p.

Rose, C. W., 1968, Water transport in soil with a daily temperature wave; Part 1, Theory and experiment: Australian Jour. Soil Research, v. 6, p. 31–44.

Rose, D. A., 1963a, Water movement in porous materials; Part 1, Isothermal vapour transfer: British Jour. Appl. Physics, v. 14, p. 256–262.

———— 1963b, Water movement in porous materials; Part 2, The separation of the components of water movement: British Jour. Appl. Physics, v. 14, p. 491–496.

Slatyer, R. O., and McIlroy, I. C., 1961, Practical microclimatology: Canberra(?), Commonwealth Sci. and Indus. Research Organization (under auspices of UNESCO), 328 p.

Stallman, R. W., 1967, Flow in the zone of aeration *in* Chow, Te Ven, ed., Advances in Hydroscience, v. 4: New York, Academic Press, p. 151–195.

van Bavel, C. H. M., 1966, Potential evaporation; the combination concept and its experimental verification: Water Resources research, v. 2, no. 3, p. 455–467.

van Hylckama, T. E. A., 1966, Evaporation from vegetated and fallow soils: Water Resources Research, v. 2, no. 1, 99–103.

.

FLOW CHARTS

Flow charts for estimating steady-state evaporation rates from bare soils

A. The main procedure

Obtain meteorological data: T_a, h_a, V_a, (Q_N) → ← Obtain data on the depths of water table

Obtain undisturbed soil cores from every distinct layer or horizon; see Richards (1954, p. 159)

Determine K_{sat} and the moisture-retention curve of each core; see p. 10, 30 and Richards (1954, p. 109–111)

From every moisture-retention curve, compute $K'(S)$ for a series of S values (always include $K'(0) = K'_{sat}$!). Use equation 7 and p. 5–7 of Marshall (1958) with these changes: (1) substitute the constant 2.713×10^7 for 2.8×10^{-3} and (2) use $n^{-4/3}$ instead of n^{-2}. The values obtained are not K, but K', proportional to K; see p. 10

For each soil layer, plot $\log_{10}[(K'_{sat}/K')-1]$ on the ordinate against $\log_{10} S$. Draw the best straight line through the plotted points. Compute n (= the line's slope) and $S_{1/2}$ (the line's intercept with the abscissa $= \log_{10} S_{1/2}$)

No ← More than one layer ? → Yes

No branch: Plot the $E_\infty(L)$ curve, utilizing either equations 23 and 14 or equation 25; see p. 9, 15–16

Yes branch: Plot the $E_\infty(L)$ curve, utilizing the layered-soil procedure. Start with equation 34; follow with equations similar to equation 32; end with equation 30; see p. 21, 22

Compute the value(s) of E_{pot} from meteorological data, using equation 9 and equation 5 (with $h_u = 1.0$). Enter horizontal line(s), $E = E_{pot}$, on the graph already containing the $E_\infty(L)$ plot, to produce $E(L)$ relation(s), similar to relation(s) of figure 7; see p. 16, 17, 18, 28

Using the data on the actual depth of the water table, L_{act}, read the actual E value from the $E(L)$ graph

No ← Is the actual E soil limited? → Yes

Use equation 9 and equation 5 (with $E=$ the actual E) to compute h_u; see p. 4, 5, 23

Is $h_u \leq 0.8$? → Yes → Go to the subroutine for the vapor-affected case (flow chart B)

No

STOP

B. The subroutine for the vapor-affected case

Obtain data on T_1

Using $h=0.8$, calculate K_{liq} (with equations 6 and 10) and $K_{vap} = (MghD_{hv}) / RT$; see p. 4, 6, 26–27

K_{vap} of the same order of magnitude as K_{liq} ?

No → Adjust the value of h_1

Yes

For several arbitrary E values (not much different from the actual E, yielded by the main procedure), determine the corresponding L_u values (using equation 41); plot the relation between L_u and E thus obtained; see p. 26, 27

Plot the $E_\infty(L)$ curve, yielded by the main procedure (with $L = L_{act} - L_u$, where $L_{act} =$ the actual L and $L_u =$ a variable). Also plot the relation between L_u and E derived in the previous step. The intersection between these two curves determines the value of the actual E, adjusted for vapor effects; see p. 27

$L_u \ll L_u^*$?

Yes → Redetermine T_1 at smaller L_u^* : see p. 27

No

$L_u \gg L_u^*$?

No

Yes

For several arbitrary E values (not much different from the actual E, yielded by the main procedure), compute the values of h_1^* and of the corresponding L_u', using equations 42 and 43; plot the relation between L_u ($= L_u' + L_u^*$) and E, based on this computation; see p. 27

Plot the $E_\infty(L)$ curve, yielded by the main procedure (with $L = L_{act} - L_u' - L_u^*$, where $L_{act} =$ the actual L and $L_u = L_u' + L_u^* =$ a variable). Also plot the relation between $L_u = L_u' + L_u^*$ and E derived in the previous step. The intersection between these two curves determines the value of the actual E, adjusted for vapor effects; see p. 28

STOP